Solution of Multivariate Inverse Radiation Transport Problems

John Mattingly

North Carolina State University

Presented at Oak Ridge National Laboratory

1 August 2011

Introduction

Inverse transport

- *Forward* radiation transport solves for the radiation field given a definition of the radiation source terms and transport medium
- *Inverse* transport solves the problem in the reverse direction: it infers radiation source terms and transport medium properties from measurements of the radiation field

Technical implementation

- The approach I'll describe implements an *implicit* solution: the inverse problem is solved by iterative forward calculations
- The inverse transport solver basically applies nonlinear regression to 1D deterministic transport models
- It finds a transport model that is simultaneously consistent with several radiation measurements, including gamma spectroscopy and neutron multiplicity

Objective

Infer the configuration of an unknown radiation source from its measured radiation signatures

Source properties

- Isotopic composition
- Fissile mass & multiplication
- Geometric arrangement of radiating and shielding materials

Signatures

- Gamma spectrometry
- Neutron time-correlation and multiplicity counting

Applications

- Nonproliferation
- Counterterrorism
- Emergency response

Inverse Transport Solver Components

Radiation transport engine

Computes the radiation field given a *hypothesis* for the source model – some properties of the model (e.g., dimensions, isotopics) are treated as variables in a regression problem

Detector response functions

Estimate the detectors' responses to the computed radiation field – currently gamma spectrometers, gross neutron counters, and neutron multiplicity counters can be modeled

Regression solver

Iteratively modifies the source model variables until the predicted detector responses match the actual measured responses – a match is found by minimizing the difference between the calculation and measurements

Example Problem

- The gamma spectrum below exhibits features consistent with plutonium
- The spectrum can be fit (top-right) using a simple lumped-parameter model with variable isotopics, volume, shielding, and age
- This regression analysis (bottom-right) provides an approximate model of the source

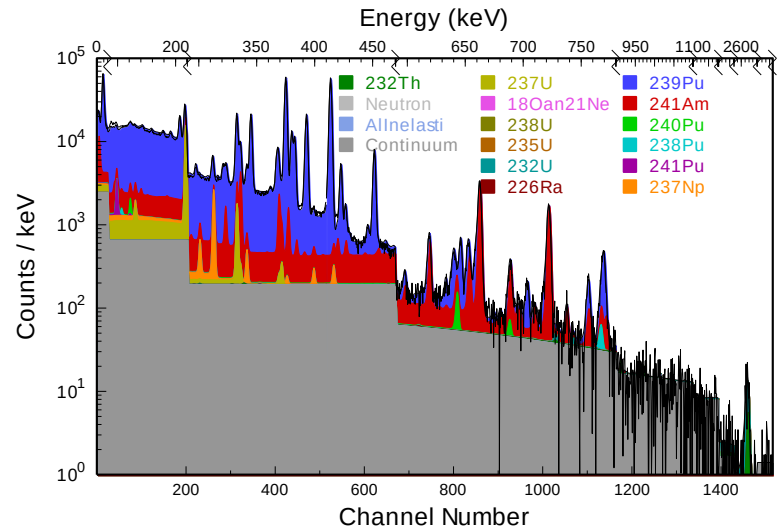

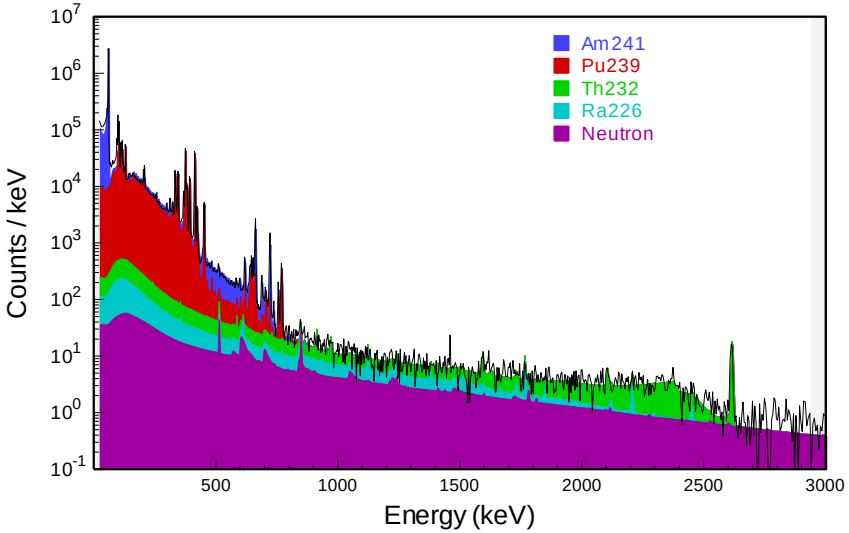


```
Plutonium wt.% (@ 33 +/-  1 years) _________ @ t=0 _________

Pu-236:    2.69E-12  +/-  1.19E-12    8.98E-09  +/-  4.75E-09
Pu-238:       0.014  +/-     0.008       0.019  +/-     0.010
Pu-239:      94.205  +/-     0.603      94.295  +/-     0.604
Pu-240:       5.279  +/-     1.157       5.298  +/-     1.161
Pu-241:       0.095  +/-     0.006       0.513  +/-     0.038
Pu-242:     [ 0.010]                   [ 0.010]
Am-241:       0.396  +/-     0.008
Np-237:       0.017  +/-     0.002
U-237:     2.94E-09  +/-  1.92E-10
U-232:     8.98E-09  +/-  3.97E-09

Confidence for measured 18O-an-21Ne gammas:        -1.6 sigma
Measured (a,n) relative to expected for oxide:     -3.0 sigma
Aluminum-inelastic peak:              1011.7 keV @  2.3 sigma
Chemical form:                                     METALLIC
External shielding:          AN = 30 +/- 1;  AD = 3.9 +/- 0.1
Outer radius if plutonium is spherical:            3.8 cm
Estimated void radius:                             3.3 cm
Estimated mass if delta-phase plutonium:           1.3 kg

There is no evidence that uranium is present.
```

1D Radiation Transport Model

- A one-dimensional transport model (top) can be generated from the regression analysis on the preceding slide
- The model shown is displayed as a section of a sphere with the center at the bottom and outer surface at the top
- The dimensions of the model layers are treated as variables for nonlinear regression

- An initial estimate of the gamma spectrum (bottom) is generated from coupled neutron-photon and electron-photon transport calculations

- Nonlinear regression can be used to find the model dimensions that minimize the error in the calculated spectrum

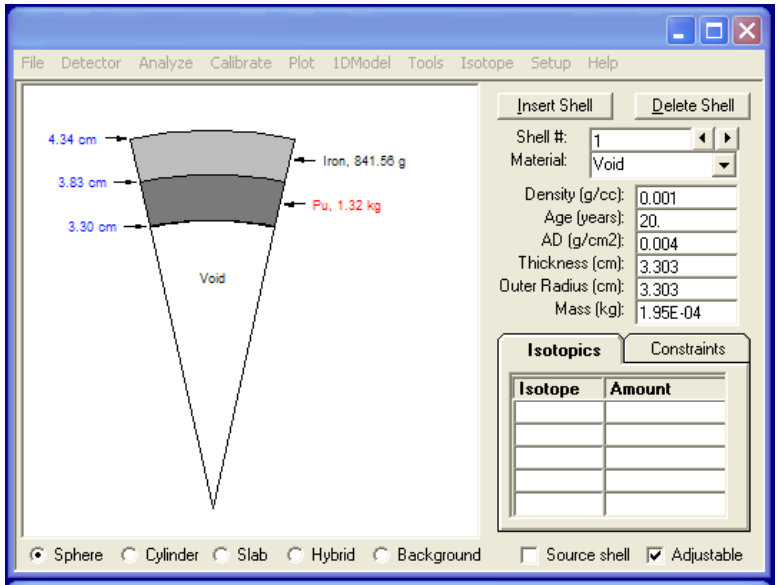

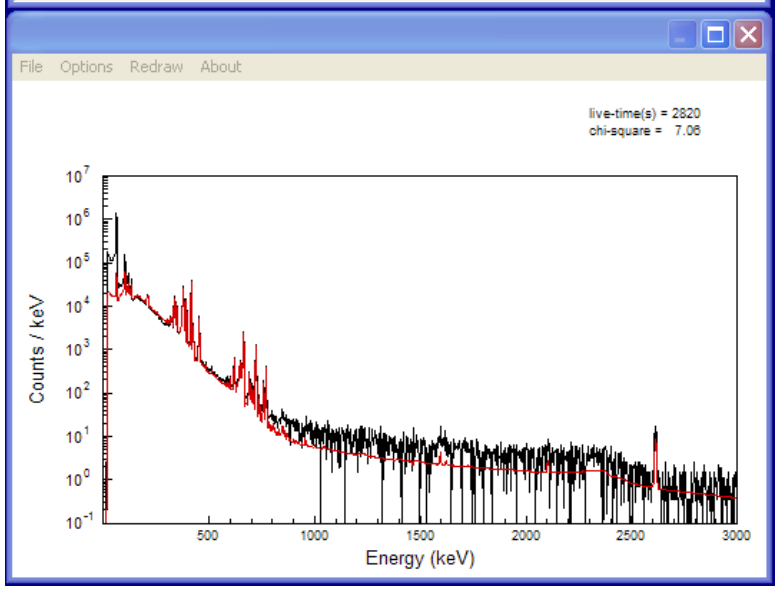

Inverse Solution

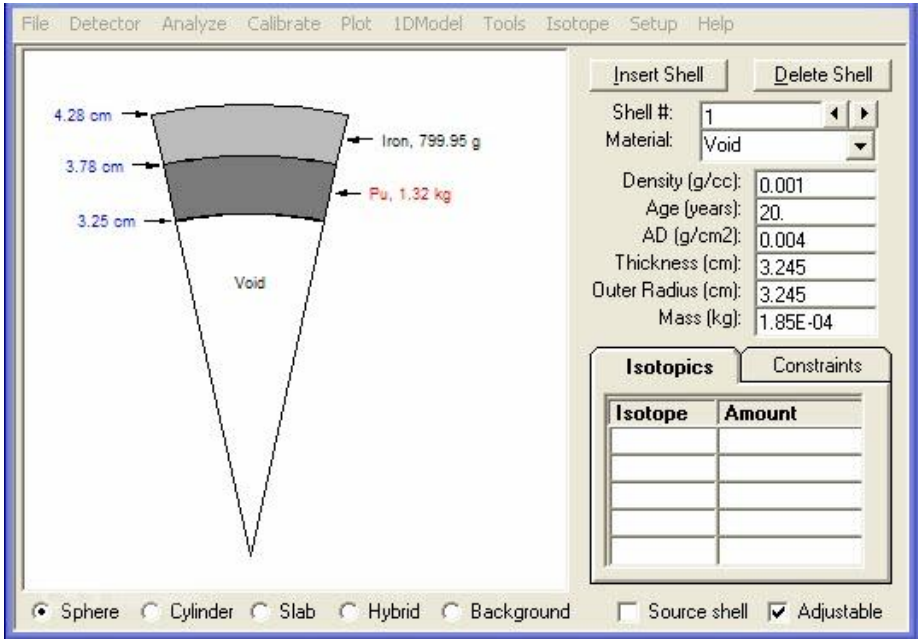

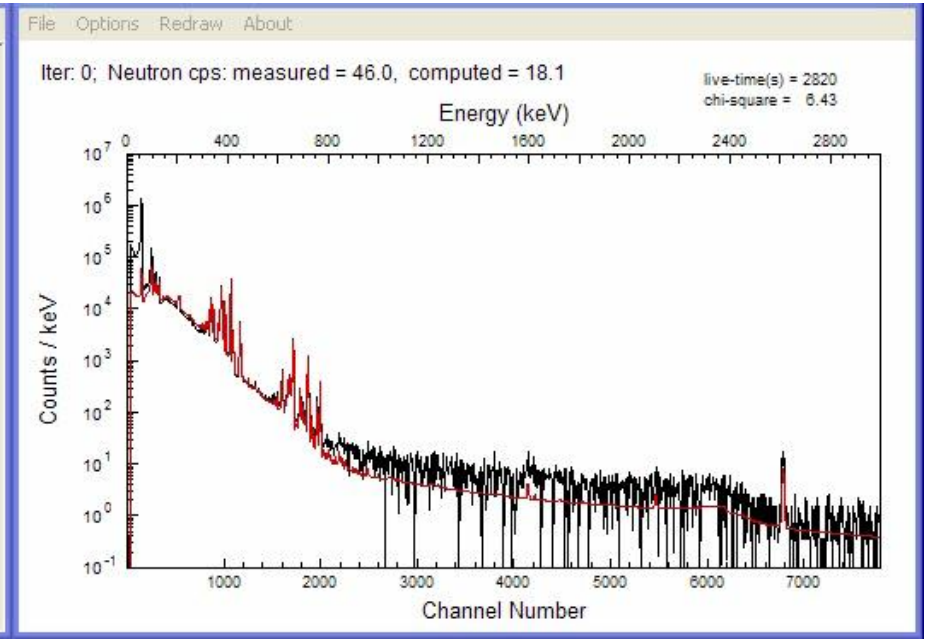

Actual Source

LLNL 2.4 kg Plutonium Sphere

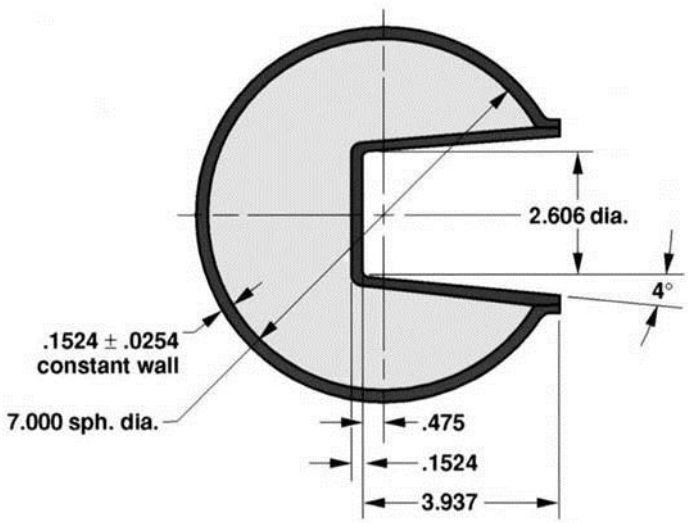

Optimized 1D Model

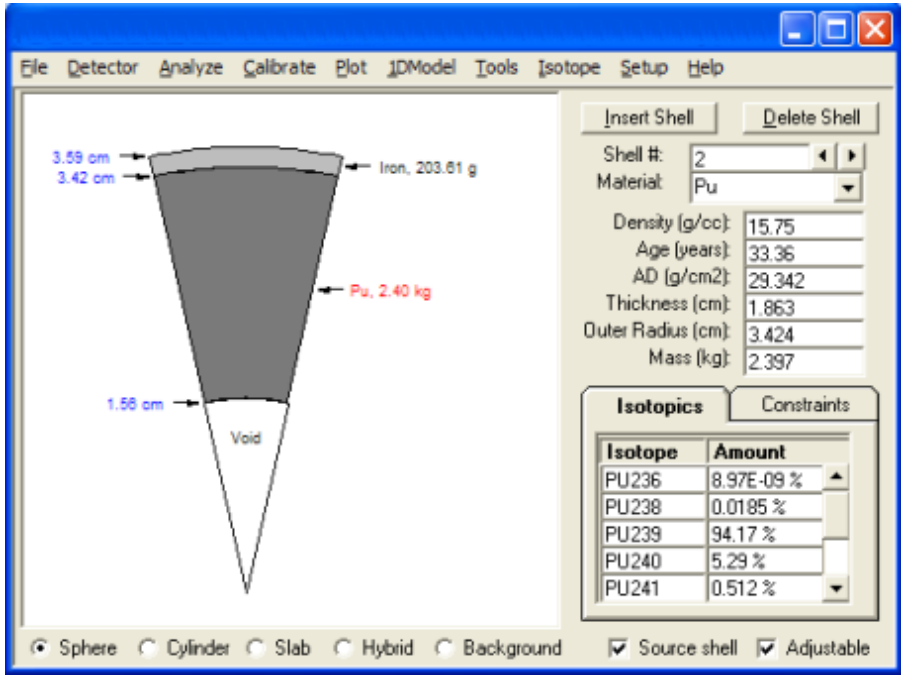

The “best-estimate” 1D model preserves the plutonium surface area and mass even though the source isn’t perfectly spherical

Solution using Gammas and Neutrons

- The gamma spectrum is primarily sensitive to the outer surface of source
- A solution based on the gamma spectrum alone is weakly constrained

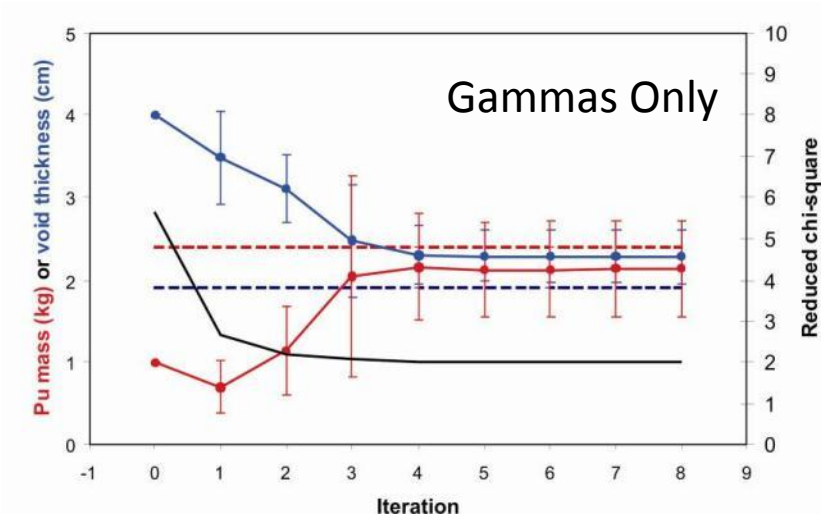

- Neutron measurements (e.g., count rate) are more sensitive to the entire volume of source
- A solution based on simultaneous analysis of gamma and neutron signatures is better constrained

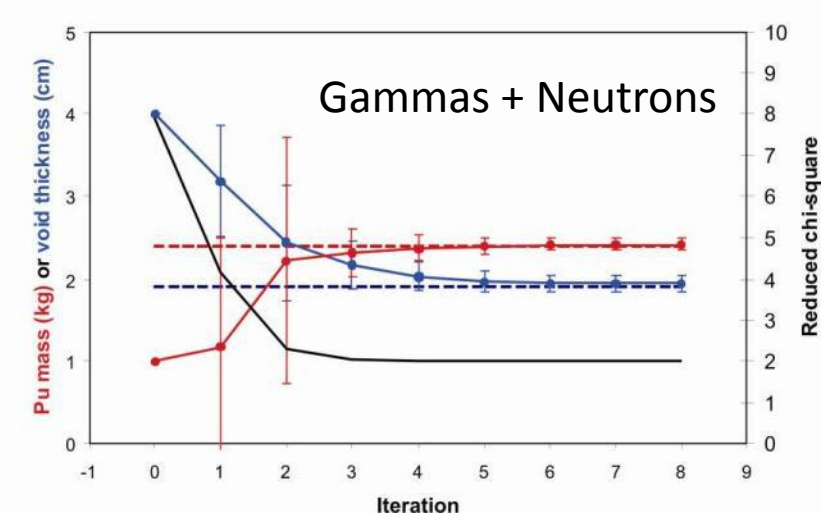

Multivariate Inverse Transport

Multivariate Inverse Transport

Gamma spectrometry analysis

- Gamma spectrometry signatures are highly specific to material isotopic composition and shielding
- But, due to self-shielding, they are mainly characteristic of the source's surface, not its volume

Neutron multiplicity analysis

- Neutron multiplicity signatures can be used to solve for fissile mass and multiplication
- However, though they are characteristic of the entire source volume, they are not highly specific to its isotopic composition

Coupled gamma/neutron analysis

- The physical phenomena governing these two observables are complementary
- They are coupled because both types of particles interact with the same medium
- A model that fits both observations is constrained to match the composition, shielding, mass, and multiplication

Gamma Spectrometry

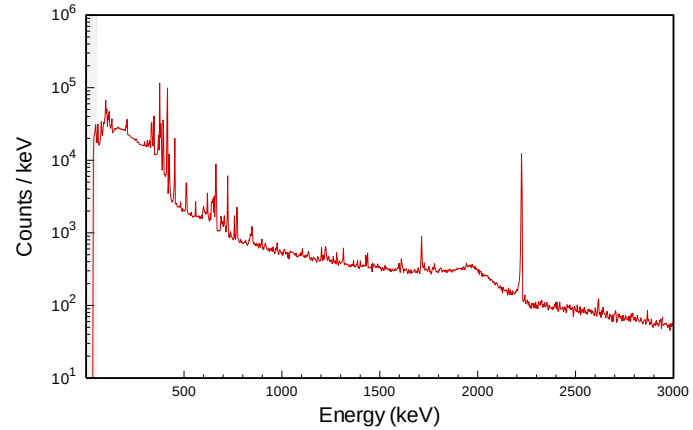

Neutron Multiplicity

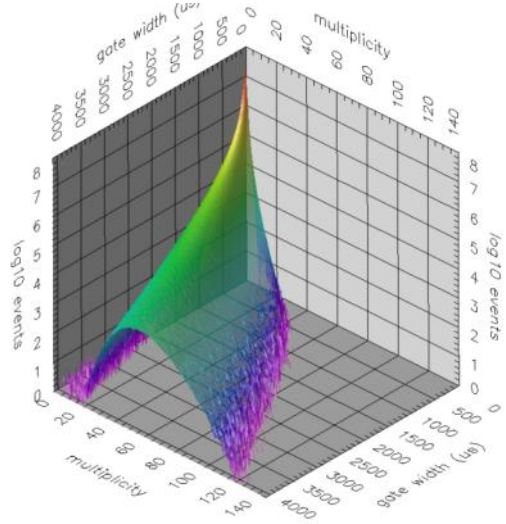

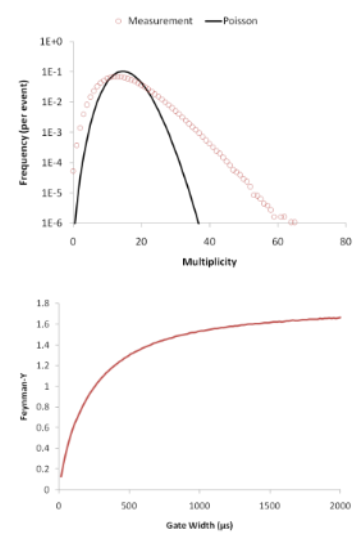

Neutron Multiplicity Counting

- Neutron multiplicity counting accumulates the distribution of detection events over:
  - Number of coincident counts (multiplicity)
  - Coincidence gate width (time)

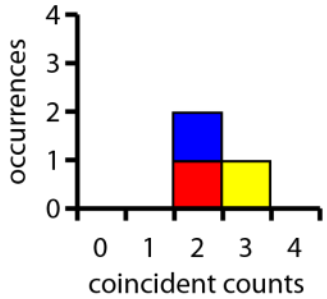

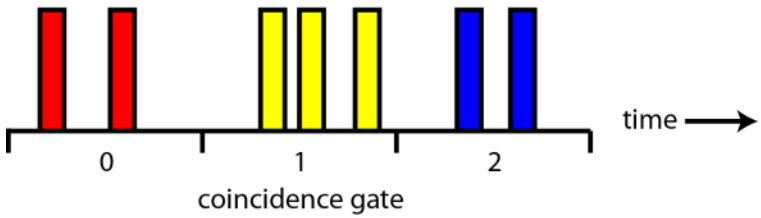

- Neutron multiplicity counting can be used to estimate kinetics parameters:
  - Source strength
  - Multiplication
  - Neutron generation time
  - Leakage probability

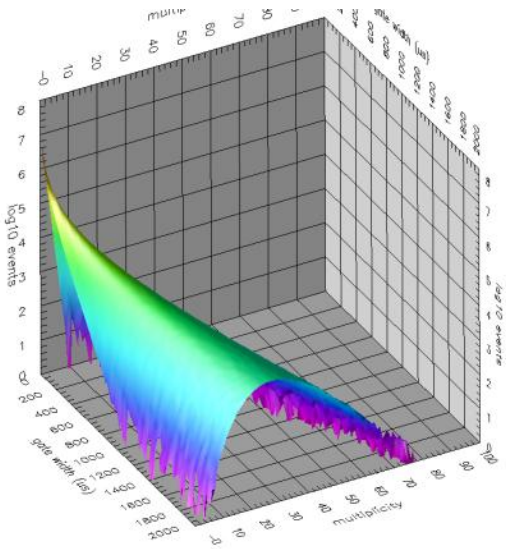

Neutron Multiplicity Distribution

Multiplication ~ 4.4
Generation Time ~ 3 ns

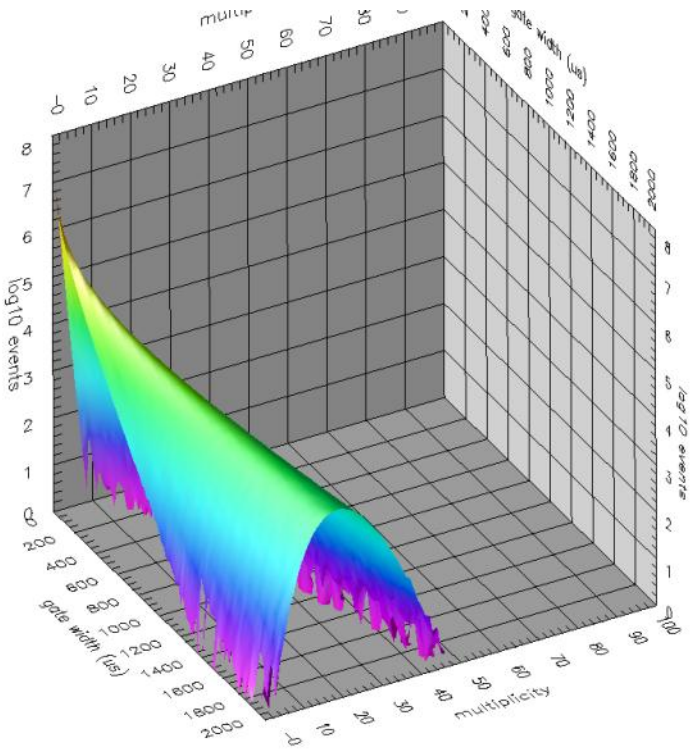

Bare 4.5 kg Pu sphere

Multiplication ~ 16.3
Generation Time ~ 9 µs

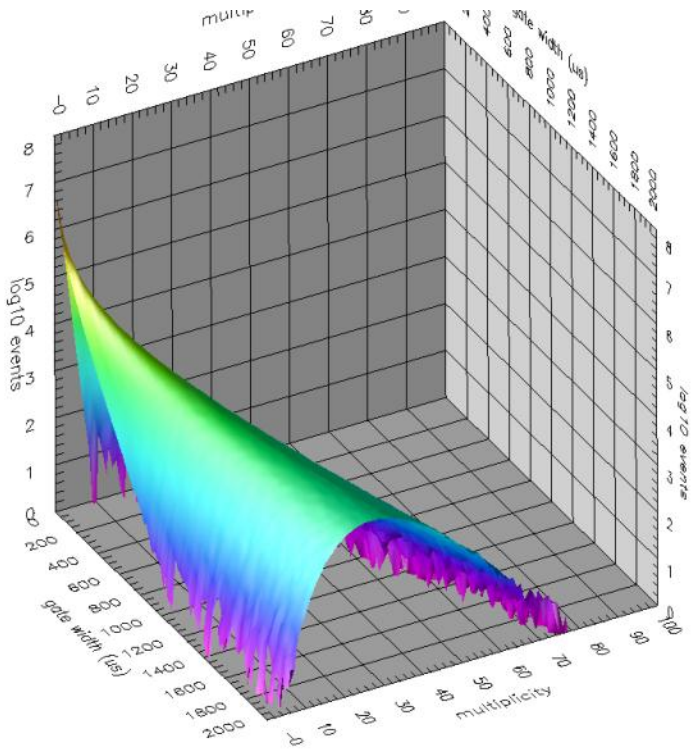

4.5 kg Pu sphere in 7.6 cm polyethylene reflector

Multiplication Produces Excess Variance

Multiplication ~ 4.4

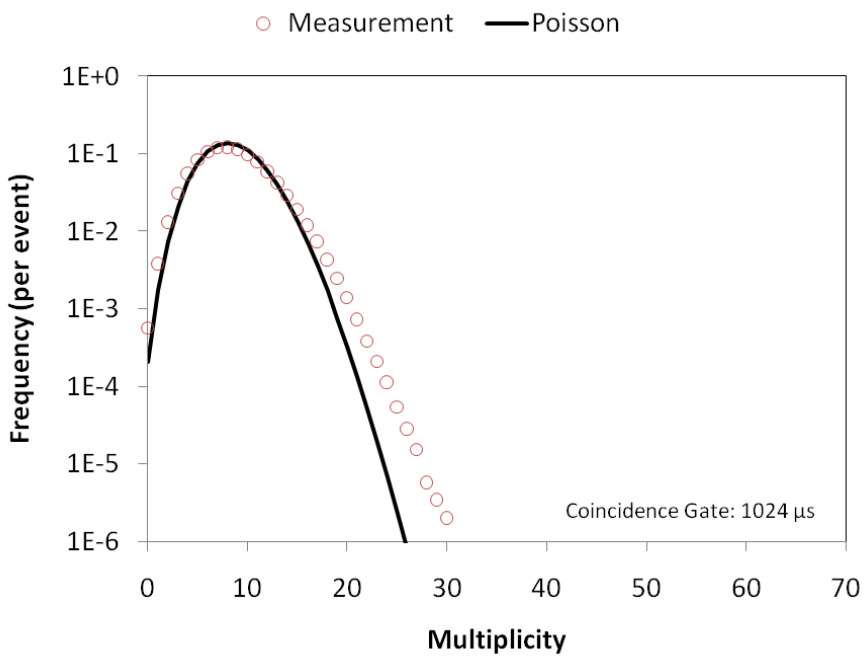

Bare 4.5 kg Pu sphere

Multiplication ~ 16.3

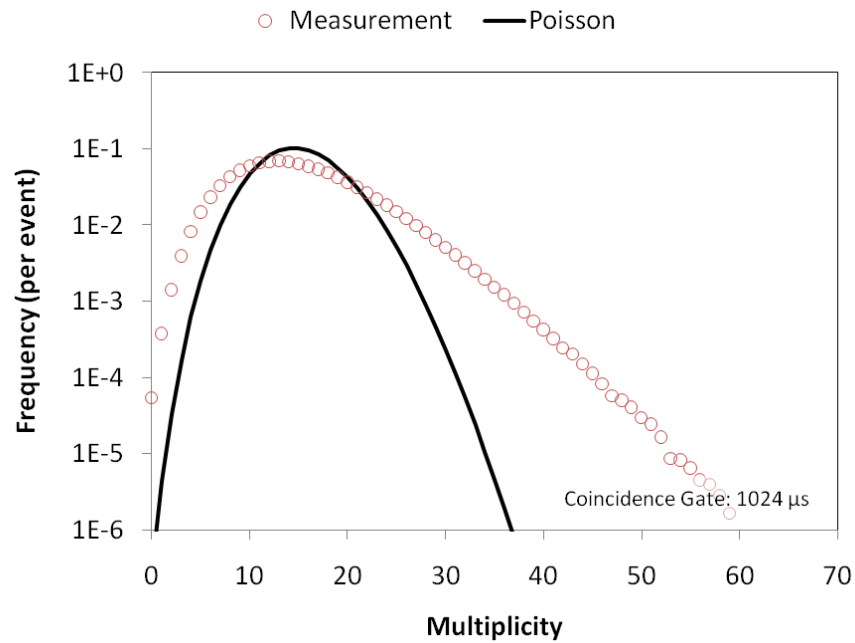

4.5 kg Pu sphere in 7.6 cm polyethylene reflector

Feynman-Y Neutron Multiplicity Statistic

- Fission chain-reactions produce "excess variance"
- The Feynman-Y measures variance in excess of a Poisson distribution

$$\frac{\sigma^2}{\mu} = 1 + Y$$

σ^2 : variance

μ : mean

  - Y vanishes if the counting distribution is purely Poisson
  - Y increases with neutron multiplication
- Y is usually measured vs. coincidence gate width

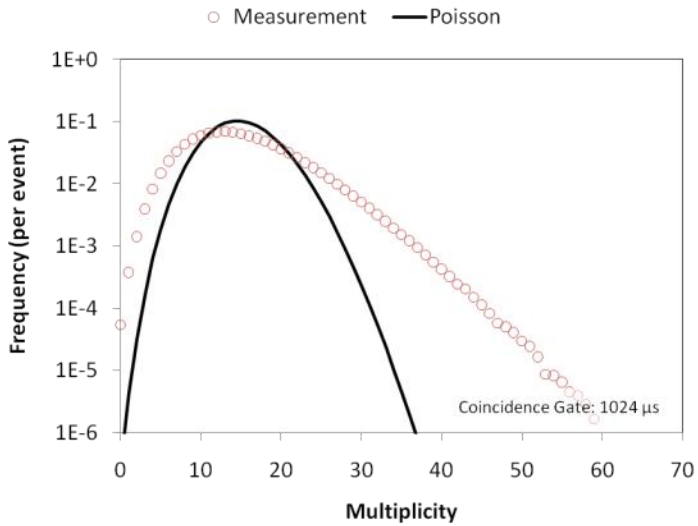

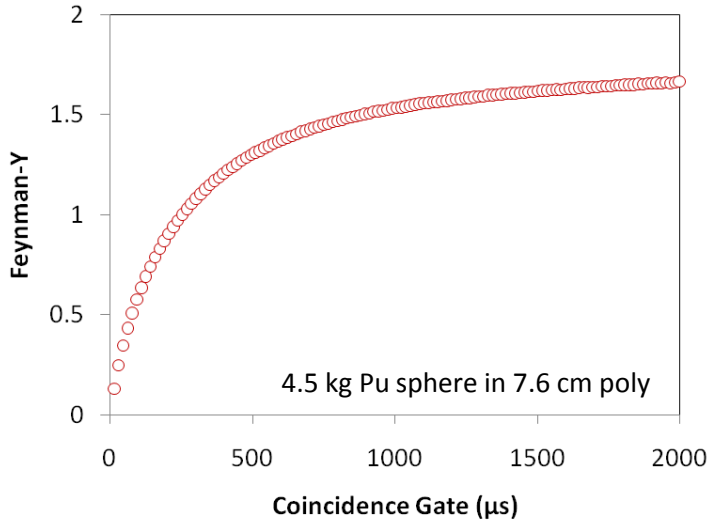

Effect of Multiplication and Generation Time

- Y is a measure of the second moment (the width) of the counting distribution
- Its asymptotic value tends to increase with square of neutron multiplication

- Y is a measure of the system's dynamic response
- Its shape vs. gate width tends to evolve more slowly with increasing neutron generation time

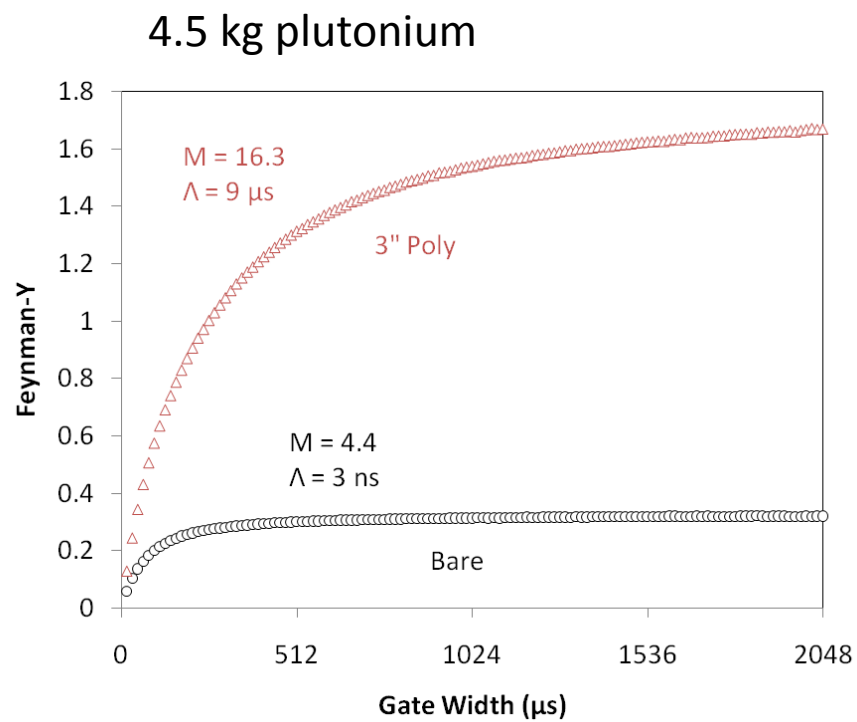

Computing Neutron Multiplicity Statistics

- There are several models for neutron multiplicity signatures
  - Point kinetics models: very fast, potentially inaccurate
  - Monte Carlo transport models: very accurate, very slow
  - Deterministic transport models: pretty fast and reasonably accurate

- I implemented a technique to compute the Feynman-Y using the same deterministic transport engine that computes the gamma spectrum
- Consequently, both the gamma spectrum and Feynman-Y can be computed from the same transport model
- So, both the gamma spectrum and the Feynman-Y can be analyzed by the inverse solver

Deterministic Computation of Feynman-Y

- Muñoz-Cobo, Perez, and Verdú developed a method to compute moments of the neutron multiplicity distribution via deterministic solution of a generalized form of the Boltzmann transport equation (see NS&E #95)

- Their method enables computation of first and higher moments (e.g., mean and variance) of the distribution using a standard S_N deterministic transport solver

- Three calculations are required
  - Forward time-independent, with the usual fixed source
  - Adjoint time-independent, the adjoint source is the detector response function
  - Forward time-dependent, with an instantaneous step in the fixed source intensity

Deterministic Computation of Feynman-Y

- Feynman-Y exhibits two notional features
  - Asymptotic value
  - Shape dependent on coincidence gate width
- Asymptote
  - Computed from static forward and adjoint transport solutions
  - Accounts for the relative contributions of source and induced fission neutrons
  - The source term for the adjoint problem is the detection response function – so, the adjoint flux “weighting function” reflects neutron “importance” to detection
- Shape
  - Computed from the solution to the dynamic forward problem where the source term is instantaneously stepped
  - The time-dependent forward flux is folded with the detector cross section and impulse response
  - The time-dependent detector response is integrated over gate width

Feynman-Y Asymptote: Excess Relative Variance

- Excess variance comes from the source and induced fission

$$\frac{\sigma^2}{\mu} = 1 + Y \qquad \sigma^2 = \mu + {}_2S_0 + {}_2S$$

- Variance due to source neutron production Q

$${}_2S_0 = \int d^3r \int dE \, \frac{\overline{\nu_0(\nu_0 - 1)}}{\overline{\nu_0}} Q(\vec{r},E) \, I_0^2(\vec{r}) \qquad I_0(\vec{r}) = \int dE' \, \chi_0(\vec{r},E') \, \varphi^\dagger(\vec{r},E')$$

- Variance due to fission neutron production $\nu\Sigma_f\varphi$

$${}_2S = \int d^3r \int dE \, \frac{\overline{\nu(\nu - 1)}}{\overline{\nu}} \nu\Sigma_f(\vec{r},E) \, \varphi(\vec{r},E) \, I^2(\vec{r}) \qquad I(\vec{r}) = \int dE' \, \chi(\vec{r},E') \, \varphi^\dagger(\vec{r},E)$$

- The importances I_0 and I are weighted by $\varphi^\dagger$, which is the solution to the adjoint transport problem using the detector response function Σ_d as the adjoint source $Q^\dagger$

Feynman-Y Shape: Dynamic Response

- The Feynman-Y shape is computed from the solution to the forward dynamic step response problem

$$Y(T) \quad \propto \quad \frac{1}{T}\int_0^T dt \int_0^t dt' \int d^3r \; h(t-t')\Sigma_d(\vec{r},E)\,\varphi(\vec{r},E,t')$$

- The time-dependent forward flux φ is computed in response to instantaneous step in forward source term Q
- The time-dependent flux is folded with the detector cross section Σ_d and impulse response h
- Then the detector response is integrated over coincidence gate width T

Step Response Calculation of Feynman-Y

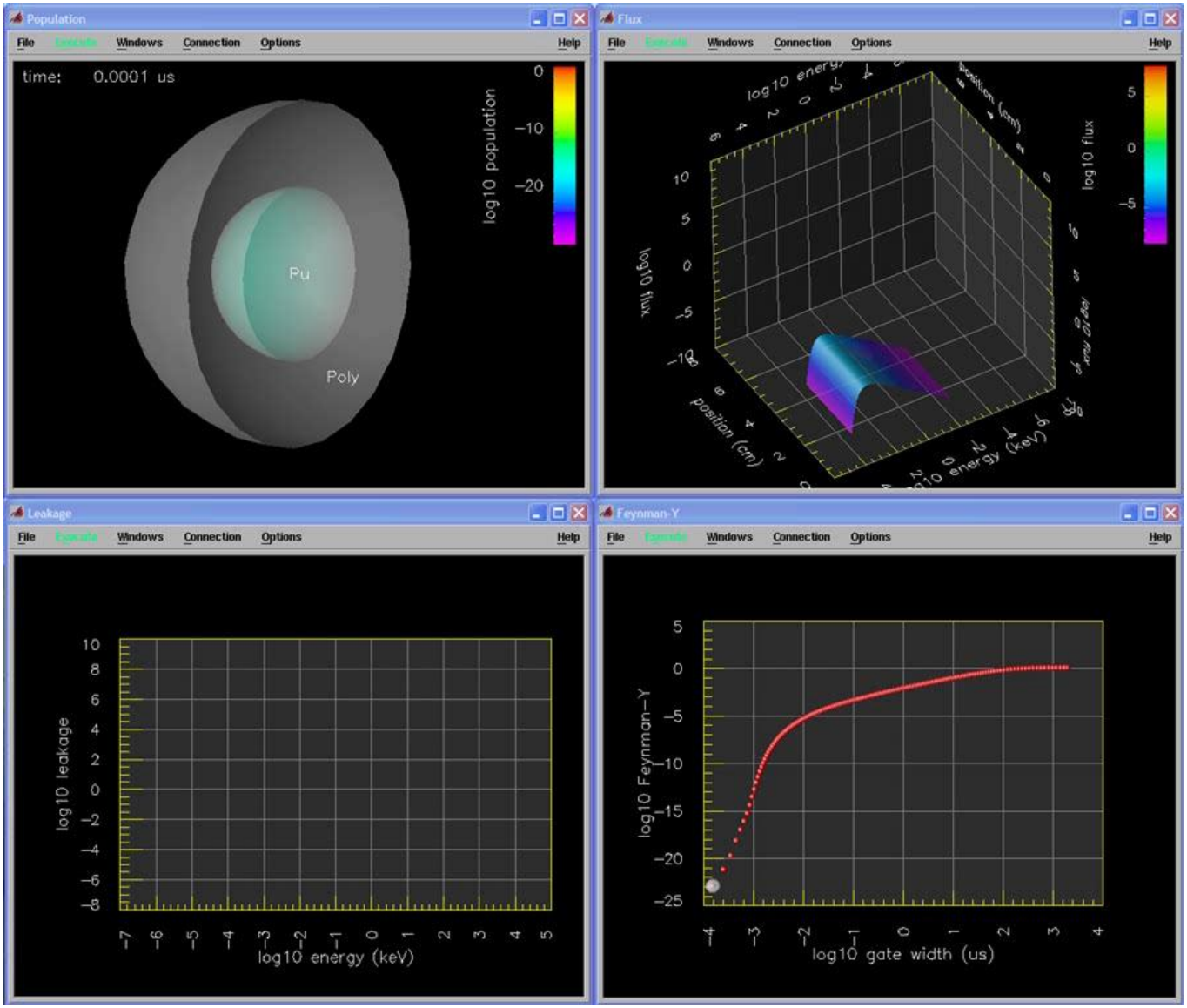

Experimental Validation

In order to validate the multivariate inverse transport solver, I conducted benchmark experiments at Nevada Test Site in January 2009

Source

- 4.5 kg weapons-grade plutonium metal sphere (the "BeRP ball")
- Reflected by polyethylene up to 6 inches thick

Detectors

- High-resolution gamma spectrometer
- Gross neutron counter (SNAP)
- Portable neutron multiplicity counter (nPod)

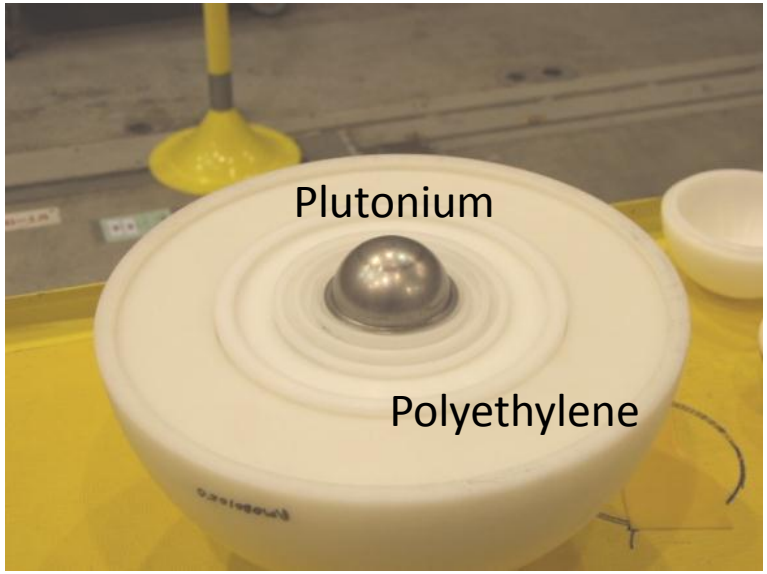

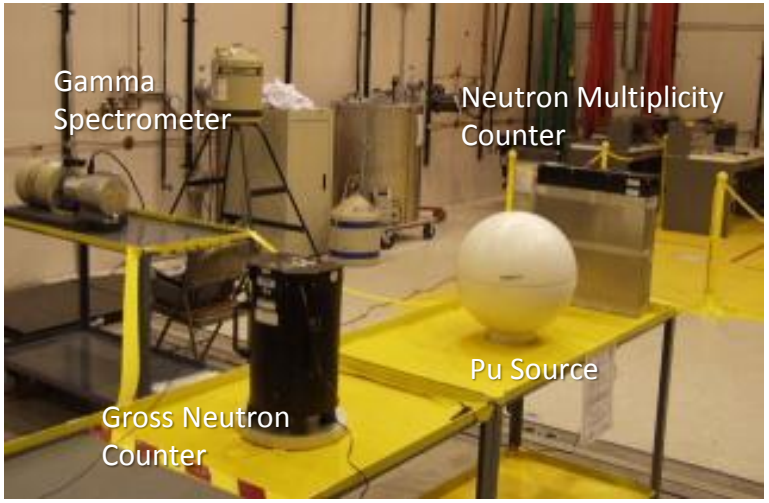

Test Source Configurations

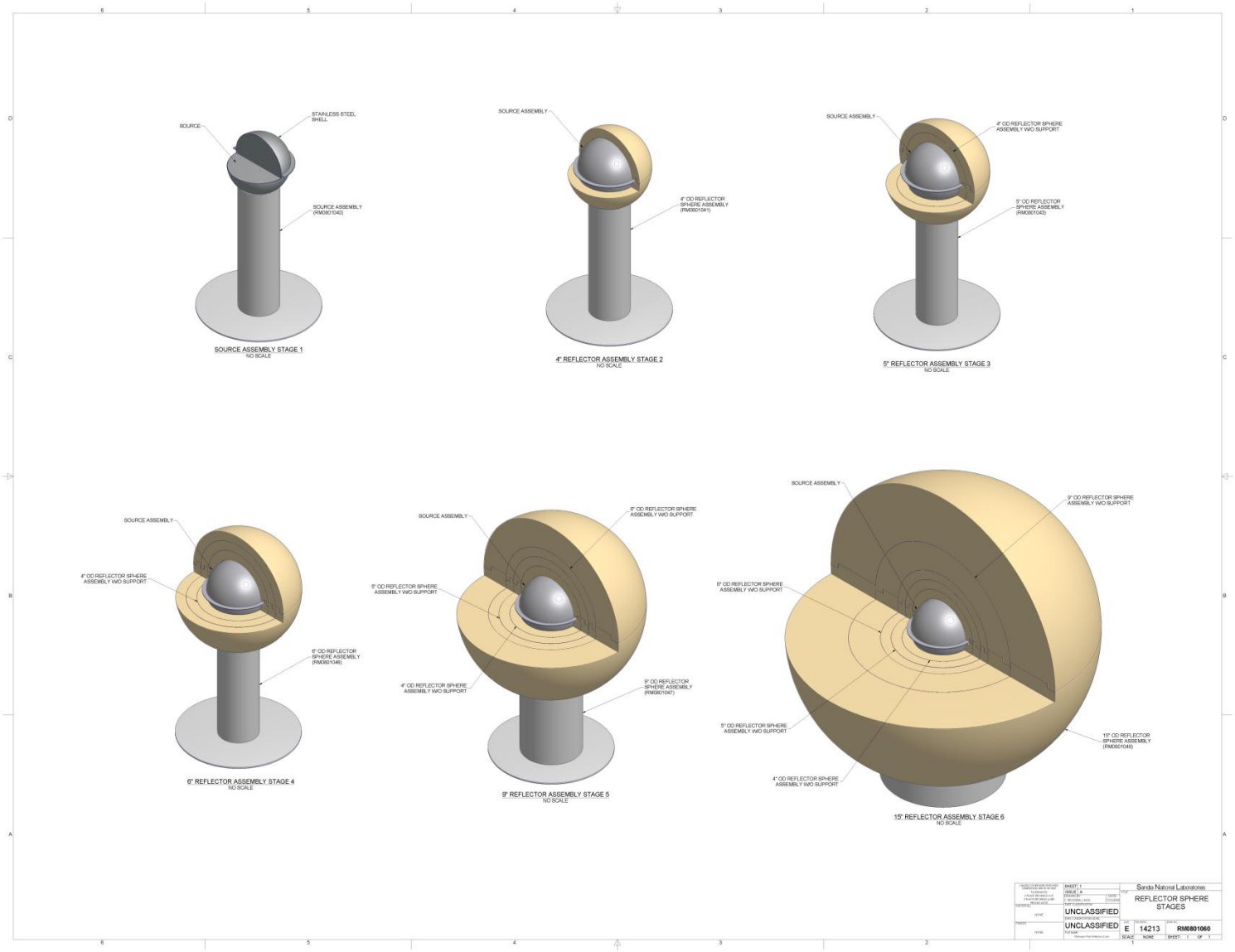

Analysis of Benchmark Experiments

- The benchmark experiments were analyzed to determine if the inverse solver would correctly infer the source configuration in each case
- The objective was to correctly estimate plutonium mass, multiplication, and reflector thickness
- Each case was analyzed with the same starting model
  - 1 kg plutonium
  - 1 cm iron
  - 1 cm polyethylene
- The solver fit the thickness of each model layer to the measurements
  - Gamma spectrum
  - Neutron count rate (with the SNAP cover both on and off)
  - Neutron multiplicity distribution variance-to-mean ratio (Feynman-Y)

Initial Guess vs. Measurement

1.5 inch Reflector

Model

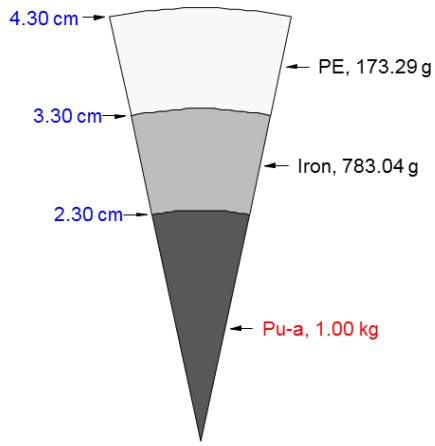

Gamma Spectrum

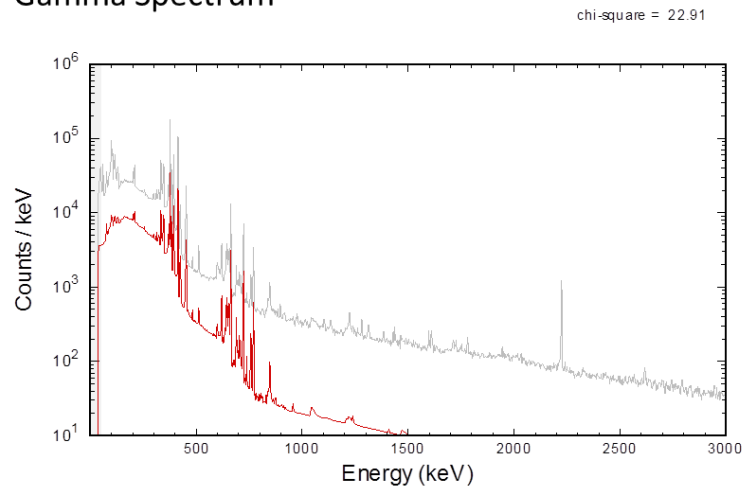

Neutron Count Rate

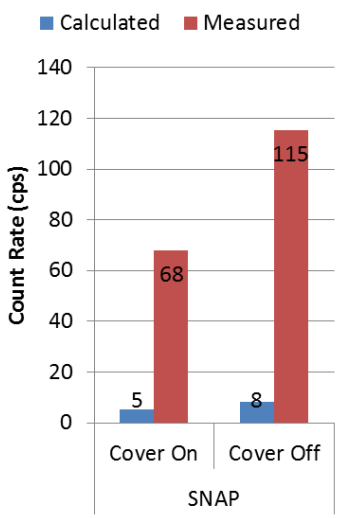

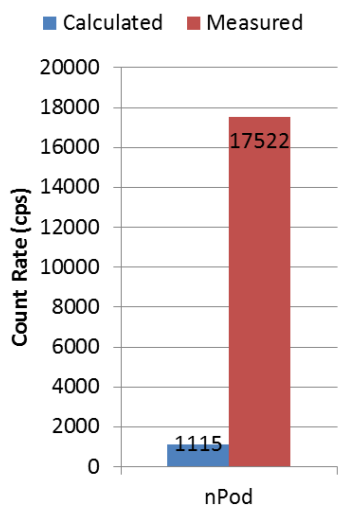

Feynman-Y

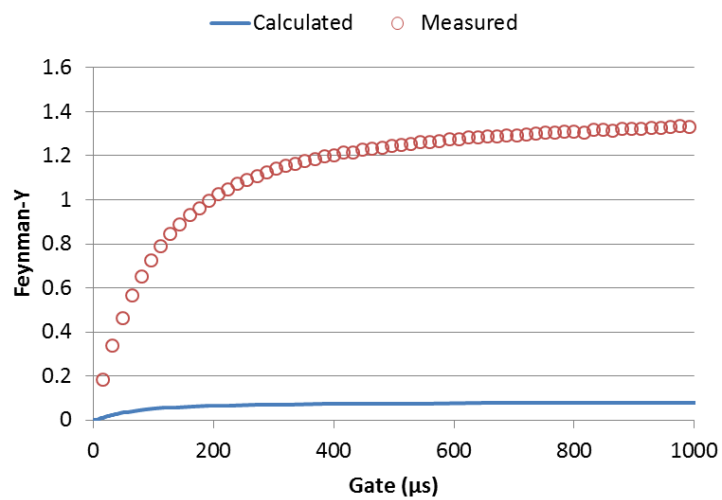

Inverse Solution vs. Measurement

1.5 inch Reflector

Model

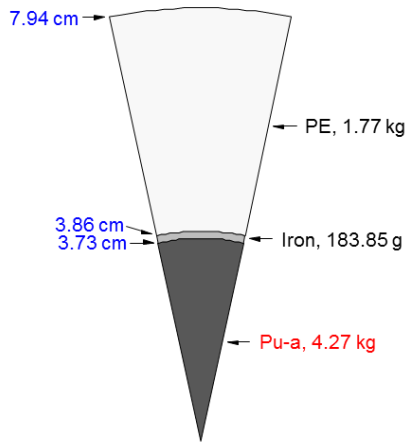

Gamma Spectrum

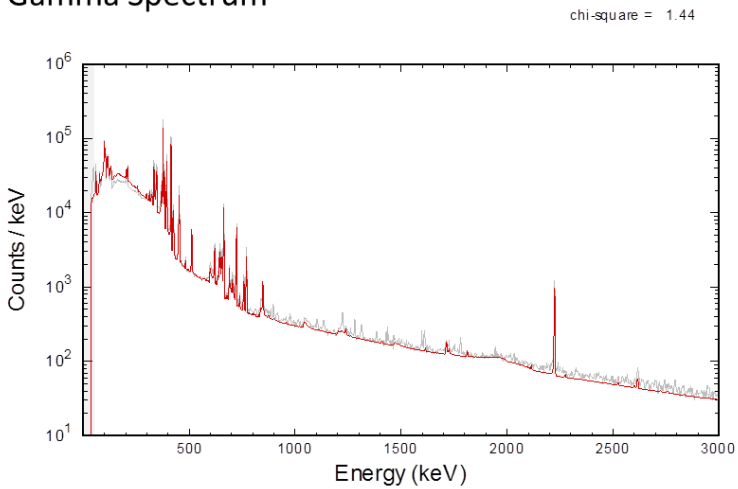

Neutron Count Rate

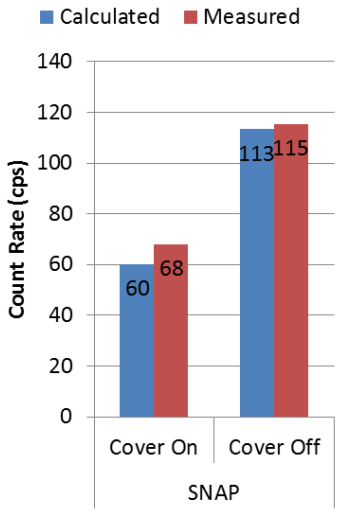

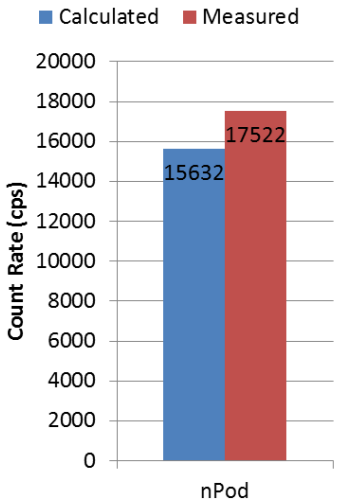

Feynman-Y

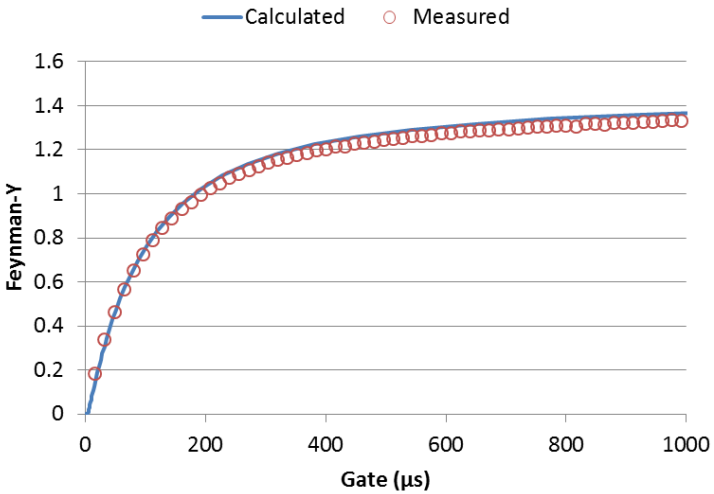

Validation Test Results

Reflector	Plutonium Mass (kg)		Neutron Multiplication		Reflector Thickness (cm)	
	Estimated	Actual	Estimated	Actual [a]	Estimated	Actual
None	4.3	4.5	4.4	4.5	N/A [b]	0.0
0.5 inch	4.6		5.5	5.8	0.8	1.3
1.0 inch	4.6		7.0	7.8	1.9	2.5
1.5 inch	4.3		9.9	10.4	4.2	3.8
3.0 inch	4.4		15.3	16.3	7.9	7.6
6.0 inch	4.4		16.4	17.1	15.0	15.2

[a] The "actual" neutron multiplication was estimated using MCNP5.
[b] For the bare case, no reflector was included in the initial model.

- The solution time was 2 minutes or less using a standard laptop
- Solution time increased with reflector thickness

Ongoing Work

Accelerating Deterministic Transport Calculations

- The most time-consuming calculation is solution of the forward time-dependent neutron transport problem

- I worked with University of Florida and Georgia Tech to develop a method to collapse neutron cross-sections using adjoint flux weighting
- It collapses energy groups in spectral regions that are “unimportant”, i.e., that contribute little to the neutron detector response

- We were able to reduce the computational time by a factor of 2

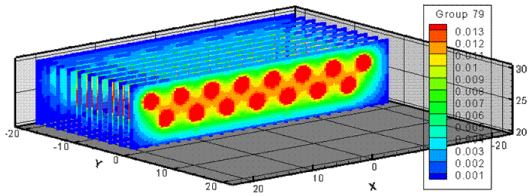

Thermal Neutron Importance

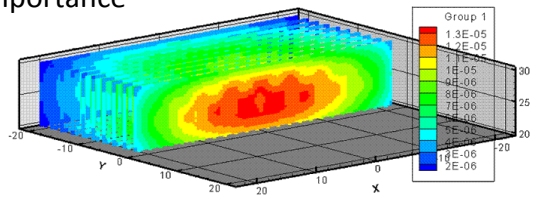

Fast Neutron Importance

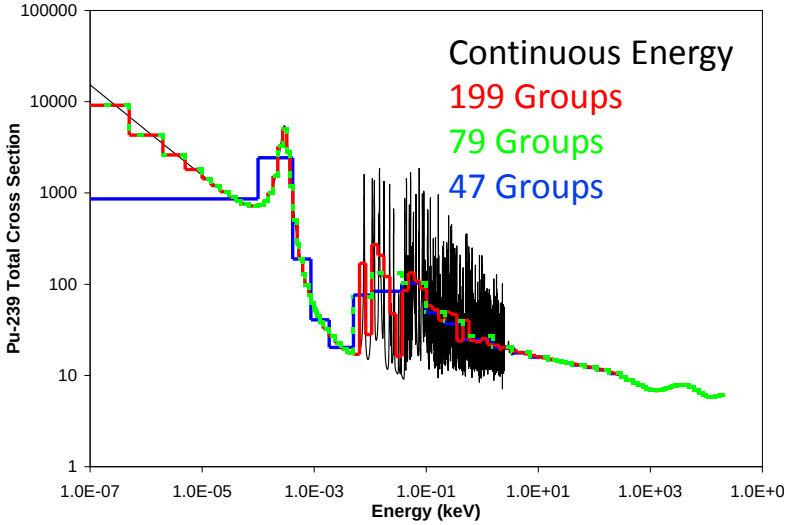

Combining Multiple Detector Responses

- Nonlinear regression minimizes the error between a model's prediction and the actual observation
- Standard regression methods employ an error metric that treats observations as if they are mutually independent
- However, errors are correlated
- Error covariance has two classes:
  - *Experimental noise covariance*: Correlation between random variations in the observation – dominates the error metric near the solution
  - *Model error covariance*: Correlation between systematic errors in the model prediction – dominates the error metric far from the solution
- My colleagues at Sandia and I developed methods to include experimental noise and model error covariance in the nonlinear regression analysis

Chi-squared error metric:

$$\chi^2 = \sum_n \frac{(f_n(\mathbf{X}) - y_n)^2}{\sigma_n^2}$$

y : observation

f : model

σ : uncertainty

$\mathbf{X}$: variables

Generalized to include covariance:

$$\chi^2 = (f(\mathbf{X}) - y)^T \boldsymbol{\Sigma}^{-1} (f(\mathbf{X}) - y)$$

$$\boldsymbol{\Sigma} = \begin{pmatrix} \sigma_{11} = \sigma_1^2 & \sigma_{12} & \cdots & \sigma_{1N} \\ \sigma_{21} & \sigma_{22} = \sigma_2^2 & \cdots & \sigma_{2N} \\ \vdots & \vdots & \ddots & \vdots \\ \sigma_{N1} & \sigma_{N2} & \cdots & \sigma_{NN} = \sigma_N^2 \end{pmatrix}$$

Effect of Accounting for Correlated Model Errors

- Simple example problem: Cs-137 shielded by lead
- Variables:
  - Cs-137 activity
  - Lead thickness

- The solution is degenerate: different solutions fit the data equally well
- Gamma emission is proportional to source strength ÷ shield thickness

- Errors in the shape of the continuum are correlated across many channels
- Accounting for error cross-correlation yields a unique solution

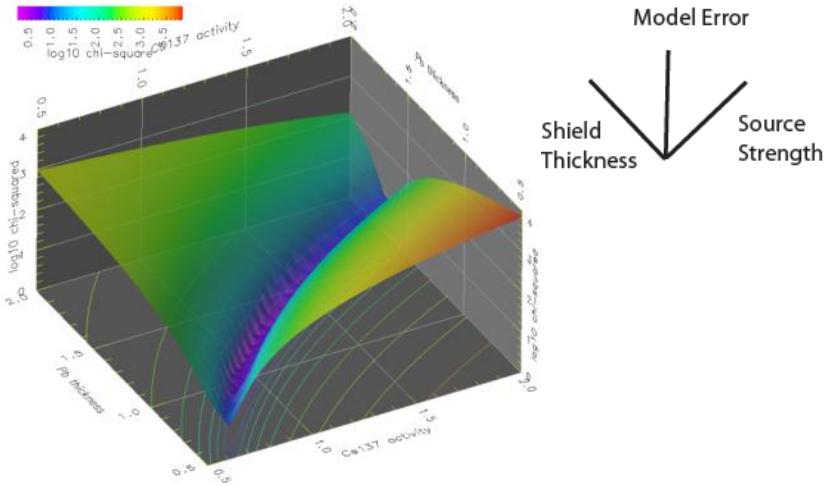

Without covariance

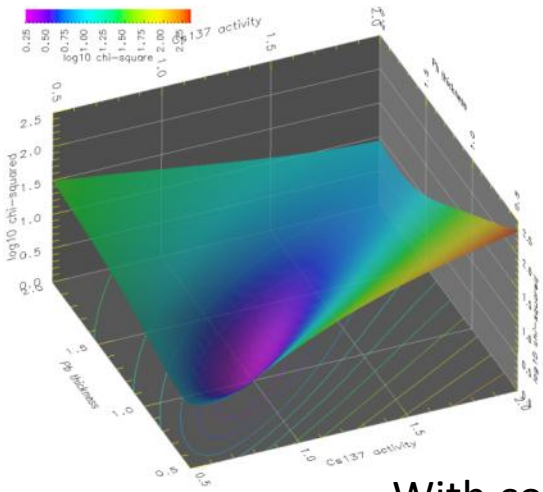

With covariance

Validating Monte Carlo Simulations

- MCNPX-PoliMi is a modification of MCNPX designed for simulation of time-correlation and multiplicity measurements
- University of Michigan and I used the BeRP ball benchmark experiments to validate MCNPX-PoliMi
- We found that MCNPX-PoliMi consistently over-estimated the measured neutron multiplicity distribution
- The over-estimation increased with neutron multiplication
- This result was independently confirmed by LANL using a different code

BeRP Ball

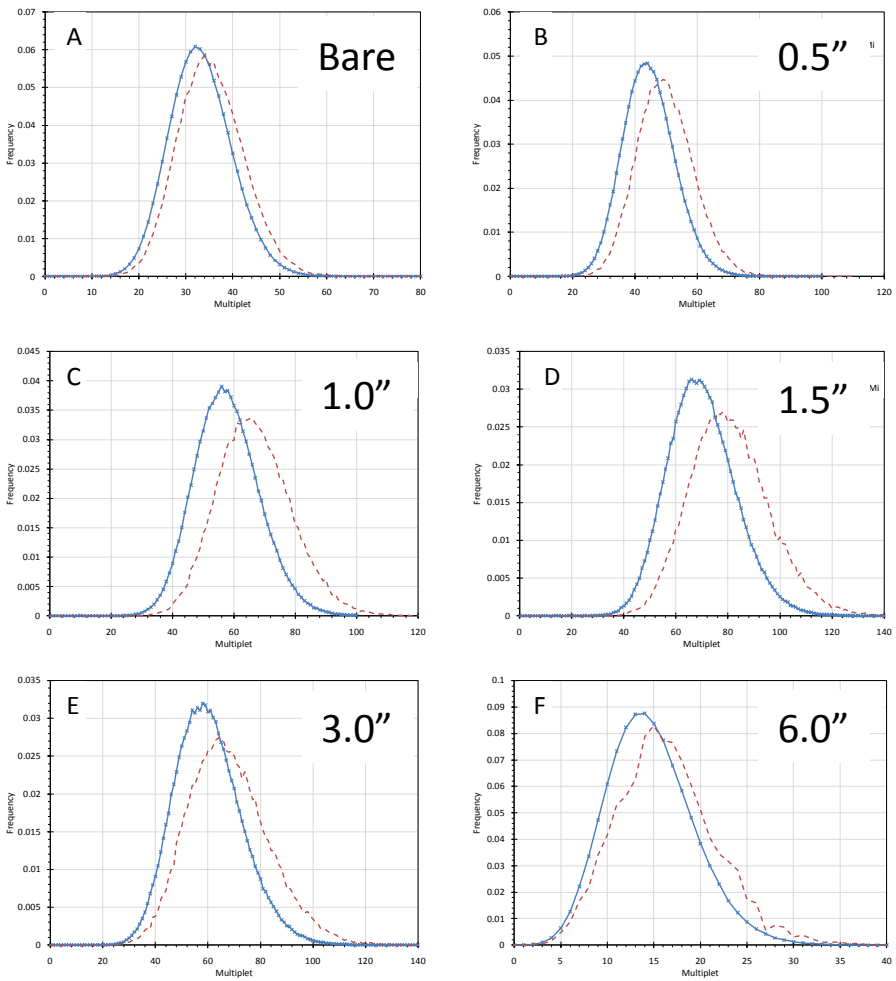

blue: experiment, red: calculation

Potential Causes of Errors

- We were able to eliminate several possible sources of error in the MCNPX-PoliMi calculations
  - Poly reflector models
  - Multiplicity counter model
  - Source-detector distance
  - Detector dead-time
  - Plutonium density

- None of these was the cause of the error

- After eliminating all the preceding possible causes, we began to investigate the nuclear data for ^{239}Pu

^{252}Cf

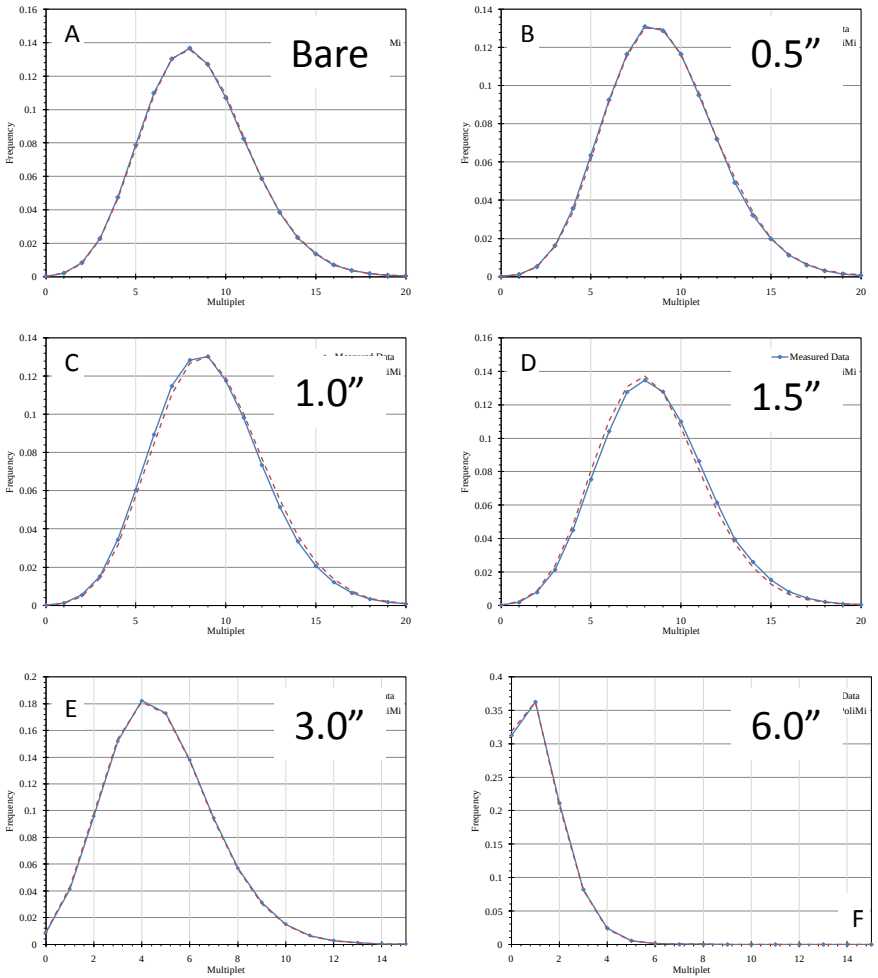

blue: experiment, red: calculation

Evaluation of Benchmark Experiments

- We found that a very small change (≈1%) in the ^{239}Pu $\bar{\nu}$ significantly reduced the calculation error in all six cases
  - The ENDF-VII evaluation of ^{239}Pu $\bar{\nu}$ is based on a single fast critical experiment – Jezebel
  - The 1% correction is comparable to the uncertainty in the ENDF-VII evaluation of ^{239}Pu $\bar{\nu}$
  - We've briefed ICSBEP and NCSP on our findings, and we've contacted the ^{239}Pu evaluation committee

BeRP Ball

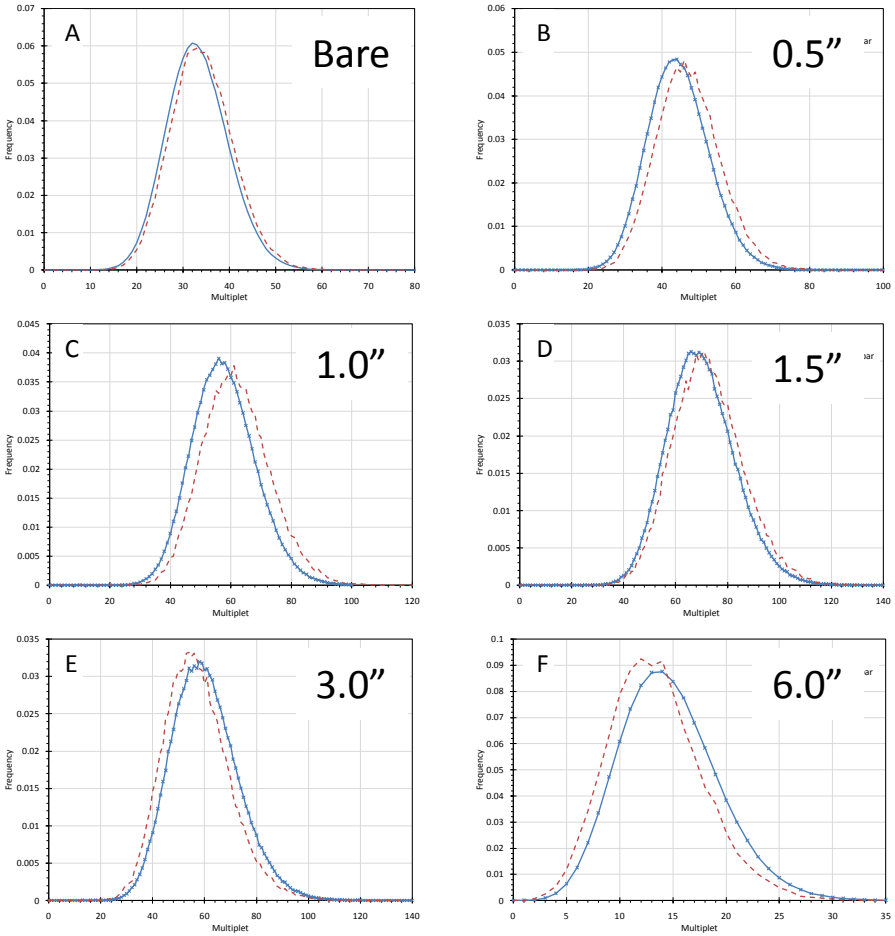

blue: experiment, red: calculation

Conclusion

Summary

- Inverse radiation transport methods can be applied to infer the configuration of an unknown radiation source from its measured signatures
- The inverse solver presented in this talk employs 1D deterministic transport models and point detector response functions embedded in a nonlinear regression solver
- The solution produces a “best-estimate” model of the source that is consistent with the measured radiation signatures
- The inverse solver is capable of combining the analysis of multiple complementary and correlated measurements, e.g., gamma spectrometry and neutron multiplicity counting
- It has been validated against benchmark experiments with special nuclear material

Future Work

- Extend the solver framework to enable a more general treatment of the forward calculations
  - Handle alternative model forms
  - Introduce new types of model variables
  - Employ alternative forward transport solvers
  - Analyze new types of detectors and observables

- Investigate different types of inverse solvers
  - Alternative gradient estimators (e.g., ones that use an adjoint solution to estimate sensitivity)
  - Derivative-free solvers for discrete variables
  - Bayesian inference solvers that produce a solution that is characterized by a distribution on the variables, instead of a single best estimate

- Evaluate the stability of the inverse solution

Acknowledgements

- The bulk of this work was performed at Sandia National Laboratories by my colleague Dean Mitchell and me.
- Sandia National Laboratories is a multiprogram laboratory operated by the Sandia Corporation, a wholly owned subsidiary of the Lockheed Martin Company, for the United States Department of Energy's National Nuclear Security Administration (NNSA) under contract DE-AC04-94AL85000.

- Development of the inverse transport solver was funded in part by the NNSA Office of Nonproliferation Research and Development.

- The benchmark experiments at NTS were funded in part by the NNSA Nuclear Criticality Safety Program.

Supplemental Slides

Radiation Transport Engine

The radiation transport engine performs deterministic coupled neutron-photon and electron-photon transport calculations to estimate:

- Neutron leakage current from:
  - Spontaneous fission
  - (α, n) reactions
- Discrete and continuous photon leakage current from:
  - Radioactive decay (i.e., α, β^-, β^+/EC, IT, IC, etc.)
  - Neutron capture and inelastic scatter
  - Spontaneous and induced fission and (α, n) reactions
  - Electron-bremsstrahlung
  - Fluorescence x-rays

- PARTISN solves the neutron transport problem
- ONELD solves the photon and electron transport problems

- The transport models are restricted to one spatial dimension
  - The solver is designed to analyze a single gamma spectrum; it's hard to infer a unique model geometry with more than one dimension from a single spectrum
  - The solver is designed to permit inexpert users to rapidly create and optimize a model

Detector Response Functions

Point detector response functions transform the neutron and photon current impinging on the detector to a computed response

Gamma spectrometers

- Solid angle
- Material (photoelectric capture, Compton scatter, and pair production probabilities)
- Detector size and shape
- Energy calibration and resolution
- Shielding and filters
- Near- and far-field scattering

Gross neutron counters

- Solid angle and intrinsic efficiency

Neutron multiplicity counters

- Solid angle and intrinsic efficiency
- Dynamic response
- Requires additional solution of adjoint and dynamic forward neutron transport problems

Regression Solver

A Levenberg-Marquardt (LM) regression solver iteratively modifies the transport model variables (e.g., dimensions, isotopic composition) to minimize the difference between the calculated and measured detector responses

Error metric

$$\chi^2 = \sum_{n=0}^{N} \frac{(y_n - \hat{y}_n)^2}{\sigma_n^2} + \sum_{p=0}^{P} \frac{\left(x_p - \hat{x}_p\right)^2}{\sigma_p^2}$$

- Variance-weighted sum of squared errors between model and experiment (1st term)
- Constraints are implemented by penalizing the cost function when a variable deviates significantly from a user-assigned nominal value (2nd term)

Gradient estimation

- The local gradient is estimated by forward difference calculations that perturb each variable; requires P + 1 transport calculations per iteration

Stopping criteria

- The solver runs for a fixed number of iterations; it can be stopped by the user

Forward vs. Adjoint Flux

- Forward transport: rate of change = source + production – losses

$$\frac{1}{\mathrm{v}}\frac{\partial}{\partial t}\varphi \quad = \quad Q \quad + \quad \mathbf{P}\varphi \quad - \quad \mathbf{L}\varphi$$

- Relationship between forward and adjoint

$$\left\langle \varphi^{\dagger}\, Q \right\rangle \quad = \quad \left\langle Q^{\dagger}\, \varphi \right\rangle$$

- Adjoint transport reverses time, direction, and change in energy

$$-\frac{1}{\mathrm{v}}\frac{\partial}{\partial t}\varphi^{\dagger} \quad = \quad Q^{\dagger} \quad + \quad \mathbf{P}^{\dagger}\varphi^{\dagger} \quad - \quad \mathbf{L}^{\dagger}\varphi^{\dagger}$$

- Adjoint flux represents importance of source neutrons to interaction embodied in adjoint source

$$Q^{\dagger} \;=\; \Sigma_x \quad \Rightarrow \quad R_x \;=\; \left\langle \Sigma_x\, \varphi \right\rangle \;=\; \left\langle \varphi^{\dagger}\, Q \right\rangle$$

Static Forward and Adjoint Solutions

Forward Flux

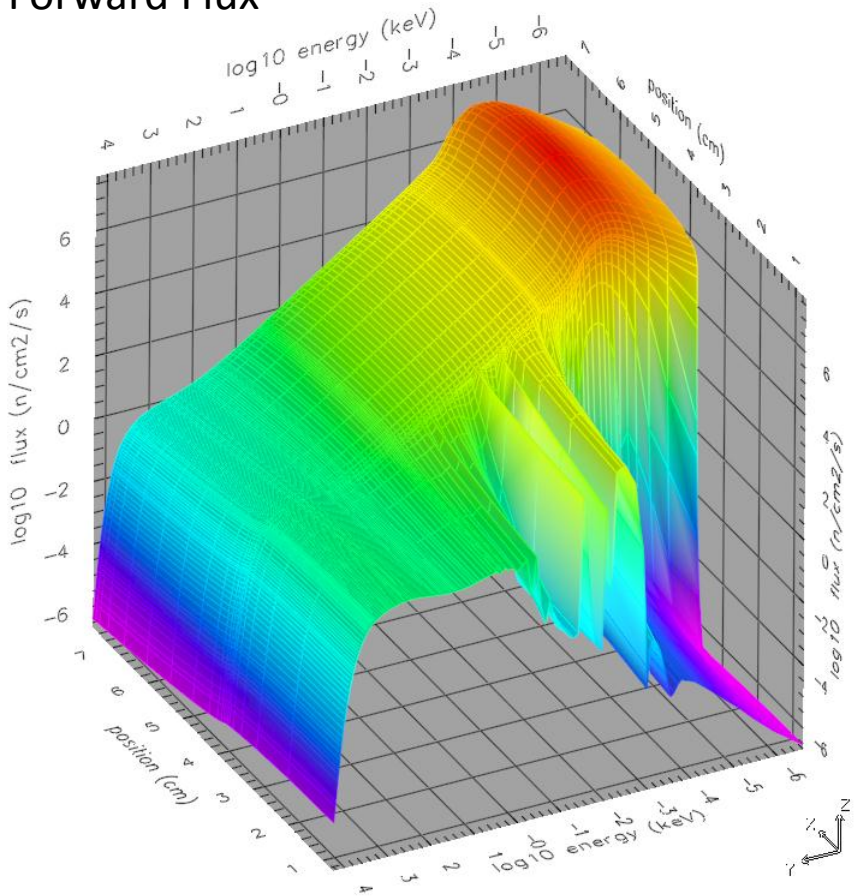

Adjoint Flux

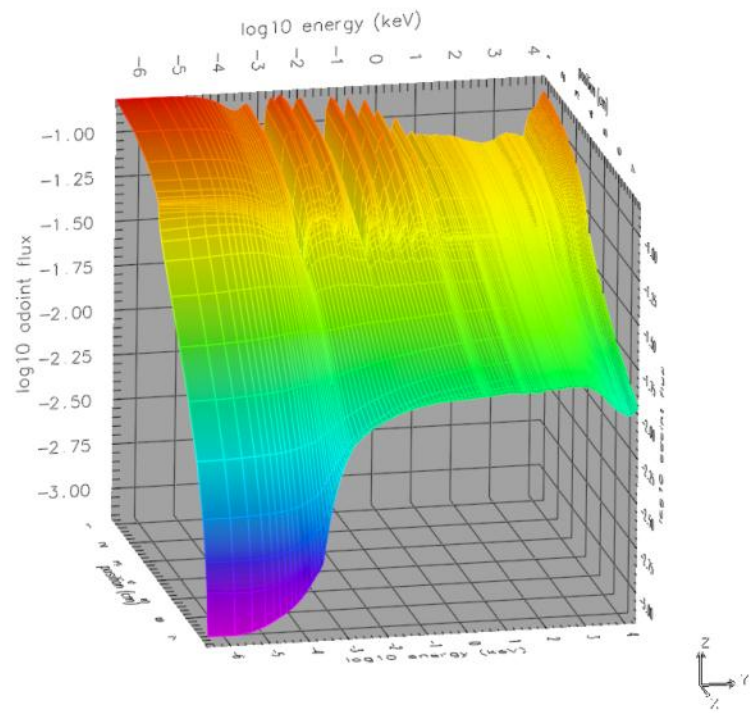

4.5 kg Pu sphere in 3.8 cm polyethylene reflector